Journal of Visualization, Vol. 8, No. 1 (2005)41-48

A study on drag reduction of a rotationally oscillating circular cylinder at low Reynolds number

Fujisawa, N.*, Ugata, M.* and Suzuki, T.*

* Department of Mechanical Engineering, Niigata University, 8050 Ikarashi 2, Niigata, 950-2181, Japan.

Received 29 March 2004
Revised 10 June 2004

Abstract : The flow field around a rotationally oscillating circular cylinder in a uniform flow is studied by using a particle image velocimetry to understand the mechanism of drag reduction and the corresponding suppression of vortex shedding in the cylinder wake at low Reynolds number. Experiments are conducted on the flow around the circular cylinder under rotational oscillation at forcing Strouhal number 1, rotational amplitude 2 and Reynolds number 2,000. It is found from the flow measurement by PIV that the width of the wake is narrowed and the velocity fluctuations are reduced by the rotational oscillation of the cylinder, which results in the drag reduction rate of 30%. The mechanism of drag reduction is studied by phase-averaged PIV measurement, which indicates the formation of periodic small-scale vortices from both sides of the cylinder. It is found from the cross-correlation measurement between the velocity fluctuations that the large-scale structure of vortex shedding is almost removed in the cylinder wake, when the small-scale vortices are generated at the unstable frequency of shear layer by the influence of rotational oscillation.

Keywords : Flow control, Vortex shedding, Circular cylinder, Wake, PIV.

1. Introduction

Vortex shedding in the wake of a circular cylinder is an important topic of interest in industrial applications of fluid mechanics. When the vortex streets are formed in the wake of the cylinder, periodic fluid forces are generated on the cylinder surface, which results in the vortex-induced vibration of the cylinder by the amplification mechanisms of vortex street at or near the natural frequency. This phenomenon is known as the synchronization of the vortex shedding and has been a topic of interest for many years.

The synchronization of vortex shedding occurs, when the circular cylinder is oscillated rotationally along the axis of the cylinder in a stream. Therefore, the synchronization of vortex shedding by the forcing at natural frequency has been studied by Okajima et al. (1975), Filler et al. (1991) and Fujisawa et al. (1998), but the studies are much less than those of linear oscillations (Griffin and Hall 1991). On the other hand, it is known that the fluid forces on the circular cylinder can be reduced by the rotational oscillation at much higher frequency of oscillation than the natural one and at larger rotational amplitude. This phenomenon is first studied by Tokumaru and Dimotakis (1991), who find drag reduction of the cylinder over 80% by rotational oscillation, which is estimated by wake velocity profile. The condition of drag reduction is found around the forcing Strouhal number Sf=1, the rotational amplitude Vr=2 at the Reynolds number Re=15,000. The drag reduction rates by numerical simulations reported in literatures are scattered in a wide range

0 - 60% at lower Reynolds number Re=1,000-3,000 (Lu and Sato 1996, He et al., 2000, Shiels and Leonard 2001, Cheng et al. 2001, Srinivas and Fujisawa 2003). Therefore, the drag reduction at lower Reynolds number is not clear. Such large scattering in the reduction rate may be due to the assumptions in computations and the flow phenomenon of laminar-turbulent transition in boundary layers.

The purpose of the present study is to investigate experimentally the flow field around the rotationally oscillating circular cylinder in a uniform flow under the condition of drag reduction at lower Reynolds numbers. For this to be done, mean and phase-averaged PIV measurements are introduced into the flow fields to confirm the drag reduction and the corresponding mechanism of flow field around the rotationally oscillating cylinder.

2. Experimental Apparatus and Procedure

The experiment was carried out in a closed-circuit water tunnel of horizontal test section having a cross-sectional area of 150mm × 150mm, which has been described by Fujisawa and Takeuchi (1999). Figure 1 shows an illustration of the flow around a rotationally oscillating circular cylinder in a uniform flow. The coordinate system is chosen in such a way that the x-axis is along the flow direction, the y-axis is in the vertical direction perpendicular to the flow, and the origin is fixed at the center of the circular cylinder. A circular cylinder of d=15mm in diameter was placed horizontally at the mid plane of the test section in a flow velocity U_0=130mm/s, so that the Reynolds number Re ($=U_0 d/\nu$) is 2,000, where ν is the kinematic viscosity of fluid. It is to be noted that the flow velocity is uniform in the test section with an accuracy of 3% except for the region close to the walls of water tunnel.

The circular cylinder is supported by the bearings, which are fixed by the vertical walls of the water tunnel. The cylinder axis is connected to an AC servo motor, which oscillates the circular cylinder rotationally with sinusoidal manner. In the present experiment, the forcing Strouhal number Sf ($=fd/U_0$) was fixed to 1 and the rotational amplitude Vr ($=d\,\omega_m/2U_0$) was set to 2 to satisfy the condition of drag reduction by rotational oscillation by Tokumaru and Dimotakis (1991), where f is a forcing frequency and ω_m is a maximum angular velocity of the cylinder oscillation.

The PIV measurement of the flow around a circular cylinder was carried out using an experimental system, which consists of the CCD camera having a spatial resolution 1008 × 1018 pixels with 8 bits, the timing controller and the stroboscopes. For flow visualization purposes, small plastic particles of specific density 1.01 were added to the working fluid water as tracers. The measurements are conducted at the mid plane of the cylinder in spanwise direction and the observation area is set to 90mm × 90mm for the whole flow measurement and 30mm × 30mm for the flow measurement near the cylinder. It is to be noted that the average diameter of the tracer particles are about 50μm for the whole flow measurement and 20μm for the near cylinder measurement, so that the particles are observed about 2 pixels in diameter in the captured images for both cases. The time intervals between the sequential two images are set by the timing controller, which produces pulse signals for imaging in synchronous with the CCD camera. The time interval between the two images is set to 300μs for the whole flow measurement and 100μs for the near

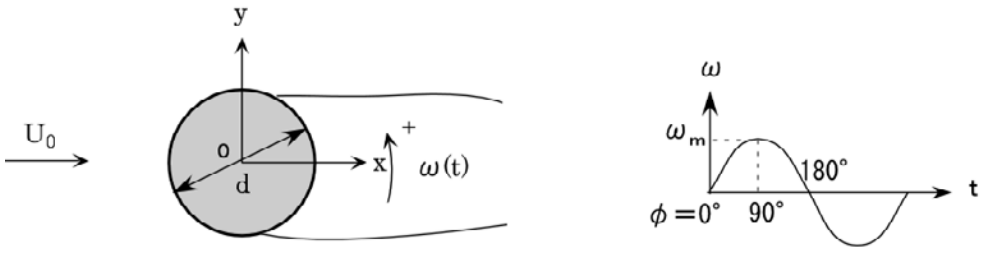

Fig. 1. Illustration of rotationally oscillating circular cylinder.

cylinder measurement, which allow the average displacement of the tracer particles 4-5 pixels in the images. The illumination is provided by white light from a stroboscope, which is introduced into the test section as a sheet of light using an optical fiber and a cylindrical lens. The thickness of the light sheet is 5mm in the test section.

When the phase-averaged PIV measurement is introduced to the flow field, the angular velocity signal from the AC servo motor is used as a timing signal for imaging, which together with the time delay set in the digital signal processor, allows the velocity measurement at the same phase of angular velocity signal (Fujisawa and Takeuchi 1998, Kim et al 2002). It is to be noted that the measurements are repeated at a fixed phase angle of angular velocity signal, which is defined by the angle φ measured from the zero angular velocity, where the angular velocity signal changes from negative (clockwise) to positive (counter-clockwise) (see Fig. 1). The phase angle was set in the digital signal processor installed to the computer, which outputs the timing signal for imaging at a certain phase lag with respect to the angular velocity signal from the AC servo motor. The uncertainty of phase angle setting is about 2°.

The instantaneous velocity fields are evaluated from the sequential two images by applying a cross-correlation algorithm (Raffel et al. 1998). The sizes of the interrogation window and the search window are set to 31×31 pixels and 15×15 pixels, respectively, which combination is found to minimize the erroneous velocity vectors with enough spatial resolution. The sub-pixel interpolation process with Gaussian-peak-fitting is also incorporated into the analysis to improve the accuracy of velocity measurement. The statistical properties of the flow field are evaluated from 300 instantaneous velocity data for both of mean and phase-averaged statistics. It is found that the uncertainty interval in the velocity measurement is found to be about 3% of the uniform flow velocity at 95% coverage.

3. Results and Discussions

3.1 Time-averaged flow characteristics

Figure 2 shows the mean velocity distribution around a circular cylinder under rotational oscillation at *Sf*=1 and *Vr*=2, which is compared with that of a stationary cylinder. The magnitude of mean velocity $\sqrt{U^2+V^2}/U_0$ is shown by color bar and the velocity direction is indicated by the arrows in this figure, where U is a streamwise mean velocity, V is a mean velocity normal to the free stream and U_0 is a free-stream velocity. The measurements are carried out at the mid span of the cylinder and at the Reynolds number Re=2,000. The mean velocity distribution of the rotationally oscillating cylinder indicates an enhancement of the local velocity on both sides of the cylinder and the reduction in the wake width behind the cylinder, in comparison with those of the stationary cylinder. Therefore, the separation points are shifted to the downstream along the cylinder surface by the influence of rotational oscillation. These results indicate the reduction in drag force acting on the circular cylinder by rotational oscillation.

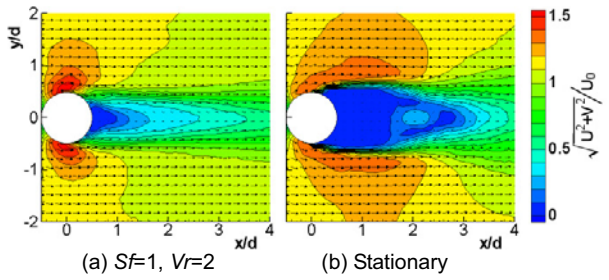

(a) *Sf*=1, *Vr*=2 (b) Stationary

Fig. 2. Mean velocity distribution.

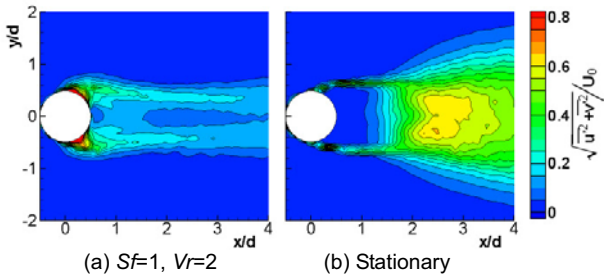

(a) *Sf*=1, *Vr*=2 (b) Stationary

Fig. 3. Fluctuating velocity distribution.

The corresponding distribution of fluctuating velocity $\sqrt{\overline{u'^2}+\overline{v'^2}}/U_0$ around the circular cylinder under the rotational oscillation is shown in Fig. 3(a), which is compared with those of the stationary cylinder (Fig. 3(b)). It is found that the velocity fluctuations in the cylinder wake is fairly reduced and the width of the wake is narrowed by the rotational oscillation of the cylinder. These changes in the fluctuating velocity distribution in the cylinder wake indicate that the vortex shedding is suppressed by the rotational oscillation of the cylinder. However, the magnitude of fluctuating velocity is increased near the cylinder surface, which may be due to the variation of separation points over the cylinder surface by the influence of rotational oscillation. It is to be mentioned that the forcing frequency of the circular cylinder at Sf=1 agrees with the effective frequency range of the shear-layer synchronization (Hsiao and Shyu 1991, Fujisawa and Takeda 2003). Therefore, the turbulent structure of the shear layer can be synchronized with the cylinder oscillation, which weakens the shear-layer interaction in the downstream of the cylinder.

The drag force D on the circular cylinder by rotational oscillation can be estimated from the momentum equation with the experimental distributions of mean and fluctuating velocities. The expression is given by the following equation (Tokumaru and Dimotakis 1991),

$$D = \int \rho\{U(U_1 - U) - (\overline{u'^2} - \overline{v'^2})\}dy \tag{1}$$

where U_1 is an undisturbed flow velocity outside the cylinder wake and ρ is density of fluid. It should be mentioned that U_1 can be affected by the blockage effect of cylinder and the boundary layer developing on the test section. Therefore, the drag force evaluated from Eq. (1) suffers from experimental errors. However, the rate of drag reduction Dr (=(D_0-D)/D_0) is less influenced by the effect, so that the drag reduction rate is directly evaluated in the present study. Here, D_0 is a drag force of a stationary cylinder and D is that of the rotationally oscillating cylinder. The drag reduction rate Dr is evaluated from the mean and fluctuating velocity distribution at x/d=3.5, 4, 4.5 downstream of the cylinder with and without rotational oscillation. The results indicate that the average drag reduction rate is found to be 30% at Reynolds number Re=2,000. The uncertainty interval in this measurement is estimated as 10% of the rate. Although the rate of drag reduction is smaller than that observed at higher Reynolds number 15,000, which is over 80% by Tokumaru and Dimotakis (1991), the drag reduction was apparently observed in the cylinder flow at lower Reynolds number Re=2,000. It is to be noted that the second term in Eq. (1) is found to be influential for evaluating the drag force, but this term is neglected in the drag-force measurement by Tokumaru and Dimotakis (1991).

3.2 Phase-averaged flow characteristics

Figure 4 shows the distributions of velocity magnitude $\sqrt{U_p{}^2+V_p{}^2}/U_0$ around the rotationally oscillating cylinder at four typical phase angles φ=0°, 45°, 90°, 135°, where U_p and V_p indicate the phase-averaged velocity in streamwise and normal direction, respectively. It is to be noted that the phase angle φ is determined by the angular velocity signal of the cylinder oscillation and the phase angle φ=0° is defined by the zero-crossing of the angular velocity signal, where the rotational direction changes from clockwise to counter-clockwise direction (Fig. 1).

Although the velocity field far from the cylinder is very similar to the mean velocity distribution in Fig. 2, the periodic variations of the flow field are clearly observed in the near wake of the cylinder. The high velocity region over the upper side of the cylinder is leaving from the cylinder to the downstream at φ=0° and it moves further downstream as the phase angle increases to φ=45°, 90°, 135°. It is also found that the high velocity region is created near the upper cylinder surface φ=45° and it moves downstream with an increase in phase angle to φ=90°, 135°. The generation of the high velocity region is expected to be due to the movement of the upper cylinder surface to the upstream by the counter-clockwise rotation of the cylinder. On the other hand, the flow over the

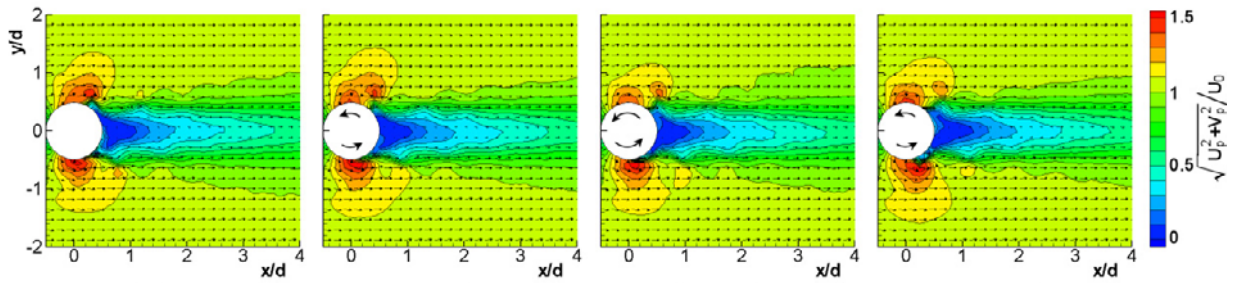

Fig. 4. Phase-averaged velocity distribution around rotationally oscillating cylinder.

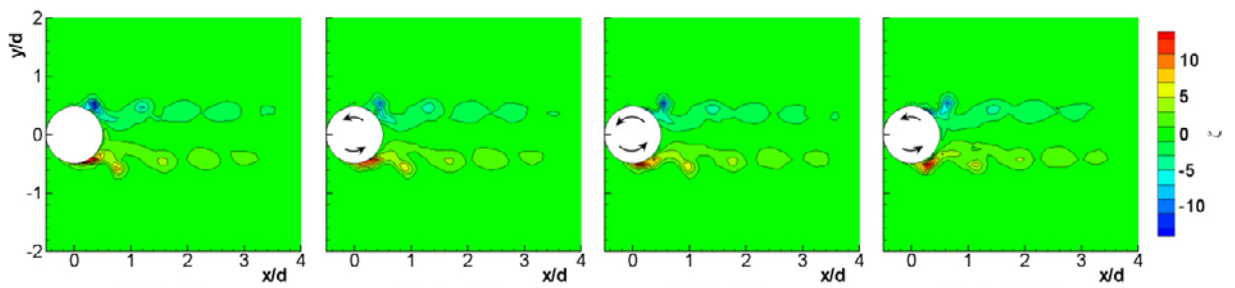

Fig.5. Phase-averaged vorticity distribution around rotationally oscillating cylinder.

lower side of the cylinder moves downward by the counter-clockwise rotation of the cylinder at φ =0° - 90°. Therefore, the low velocity region grows to the upstream on the lower side of the cylinder until it leaves from the cylinder surface at φ =135°, where the angular velocity of the cylinder is decelerated. It is to be noted that the flow field at the next half cycle of cylinder rotation φ =180° - 360° is up-side-down of the flow field of φ =0° - 180°, because of the symmetrical nature of the flow.

The corresponding distributions of phase-averaged vorticity is shown in Fig. 5 at four typical phase angles φ =0°, 45°, 90°, 135°, where the vorticity is defined by $\zeta = d/U_0(\partial V/\partial x - \partial U/\partial y)$. On the upper side of the cylinder surface at phase angle 0°, a negative vorticity is leaving from the cylinder surface and moves further downstream as the phase angle increases to φ =45°, 90°, 135°. On the other hand, the vorticity over the lower surface of the cylinder moves upstream along the cylinder surface at φ =0°-90° and leaves from the cylinder surface at φ =135°, which reflects the acceleration and the deceleration of the cylinder rotation in counter-clockwise direction, respectively. Therefore, periodic vortices are generated alternatively from the cylinder sides, which is synchronized with the rotational oscillation of the cylinder. With the advance to the downstream, these vortices form the periodic structure in the cylinder wake and develop parallel to the free-stream direction. It is to be mentioned that the variations of the vorticity field with the phase angle agree closely with those of the velocity field in Fig. 4.

3.3 Phase-averaged flow characteristics near circular cylinder

Figures 6 and 7 show the phase-averaged velocity and vorticity field near the cylinder surface, respectively, which are for four phase angles φ =0°, 45°, 90°,135°. The flow field at phase angle φ =0° shows the formation of thin boundary-layer on the lower side of the cylinder, which is due to the formation of high velocities outside the boundary layer (Fig. 6). Therefore, the positive vorticity is created near the lower cylinder surface (Fig. 7). With the advance to φ =45°, 90°, 135°, the flow over the lower side receives the influence of counter-clockwise rotation of the cylinder, which is observed in the growth of the low velocity region over the lower side of the cylinder. Therefore, the high

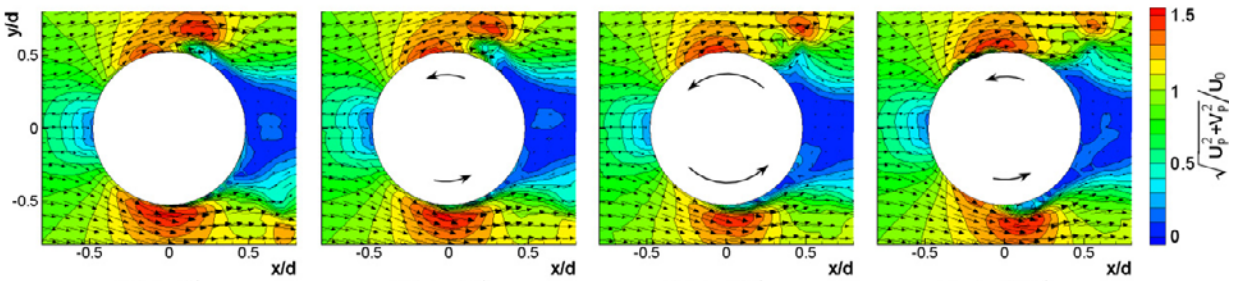

Fig. 6. Phase-averaged velocity distribution near rotationally oscillating cylinder.

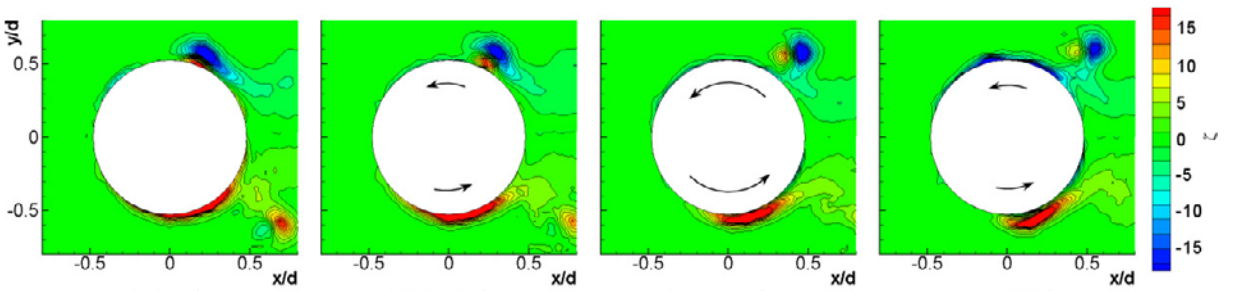

Fig. 7. Phase-averaged vorticity distribution near rotationally oscillating cylinder.

velocity region leaves from the cylinder surface and the low velocity region grows to the upstream along the cylinder surface with an increase in phase angle φ. Corresponding to this variation in velocity distribution, the positive vorticity is formed on the lower side of the cylinder at φ=135° and it grows normal to the cylinder surface. This is followed by the detachment of the vorticity from the upper cylinder surface at phase angle φ=0°, where the moving direction of the cylinder changes from the downward to the upward. However, the sign of vorticity changes from positive to negative due to the change of the flow field from the lower to the upper side. It is also found that the high velocity region is created in the upstream of the low velocity region on the lower cylinder surface at φ=135° and it moves downstream along the upper cylinder surface at φ=0°-90°, which may act to detach the negative vorticity from the cylinder surface. On the other hand, small positive vorticity is created near the upper surface of the cylinder at φ=0°. This is due to the fact that the negative vorticity is created near the lower cylinder surface, where the surface velocity is higher than the fluid velocity near the cylinder surface at φ=135°-180°. With an increase in phase angles to φ=45°-90°, such a pair of vortices detaches from the upper cylinder surface and develops into the cylinder wake in the downstream, which is consistent with the downward movement of the high velocity region along the cylinder surface in Fig. 6. Therefore, the thin boundary layer is generated over the upper surface at φ=135°, which corresponds to the formation of negative vorticity over the upper cylinder surface.

3.4 Turbulent structure in cylinder wake

The turbulent structure in the cylinder wake with and without rotational oscillation is evaluated by the cross-correlation coefficient *Ruu* between the streamwise velocity fluctuations and *Rvv* between the normal velocity fluctuations. They are defined by $R_{uu}=\overline{u'(x_0,y_0)u'(x,y)}/\sqrt{\overline{u'^2(x_0,y_0)}}\sqrt{\overline{u'^2(x,y)}}$ and $R_{vv}=\overline{v'(x_0,y_0)v'(x,y)}/\sqrt{\overline{v'^2(x_0,y_0)}}\sqrt{\overline{v'^2(x,y)}}$, respectively. The distributions of cross-correlation coefficients *Ruu* and *Rvv* in the cylinder wake with and without rotational oscillation are described in Figs. 8 and 9, respectively. It is to be noted that the reference point (x_0,y_0) is set to x_0=0.84d, y_0=0.47d in the present results, which corresponds to the upper shear layer of the cylinder wake. It

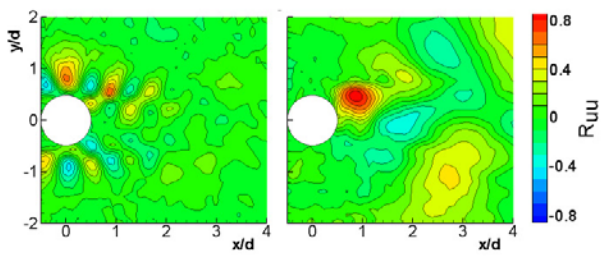

(a) *Sf*=1, *Vr*=2 (b) Stationary

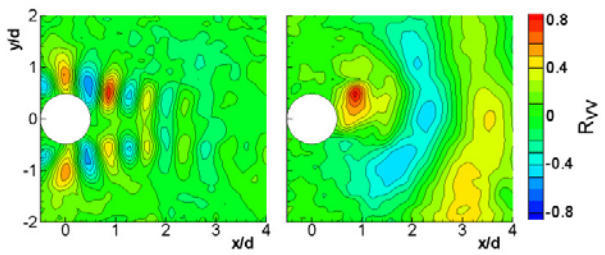

(a) *Sf*=1, *Vr*=2 (b) Stationary

Fig. 8. Contour of cross-correlation coefficient *Ruu*. Fig. 9. Contour of cross-correlation coefficient *Rvv*.

can be seen from the results of rotationally oscillating cylinder that the cross-correlation coefficients *Ruu*, *Rvv* show the small periodical structure in the cylinder wake, which is different from the large periodical structure of the stationary cylinder. The peak values in the correlation are formed along the shear layer of the cylinder wake, which develops from the high velocity region on the cylinder side toward the centerline of the wake in the downstream. It is interesting to note that the opposite sign of correlation is generated in *Ruu* and the same sign of correlation is found in *Rvv* on both sides of the cylinder at the same streamwise position *x/d*. The former is caused by the movement of the cylinder surface in opposite direction on each side of the cylinder by rotational oscillation and the latter is due to the geometrical symmetry of the flow about the flow axis. Therefore, these distributions of correlation indicate that the asymmetrical velocity field is formed on each side of the circular cylinder, which is consistent with the formation of small-scale staggered vortices as observed in Figs. 6 and 7. It should be mentioned that the high correlation values are found only near the rotationally oscillating cylinder and their magnitudes decrease in the downstream, which indicates the disappearance of small-scale vortices in the cylinder wake.

These cross-correlation contours with and without rotational oscillation indicate that the large-scale structure in the wake of the stationary cylinder is almost suppressed by the injection of small-scale vortices to the cylinder wake by rotational oscillation of the circular cylinder. Therefore, the reduction of the drag force on the circular cylinder in the present experiment is consistent with the modification of the wake structure.

4. Conclusion

The flow field around a rotationally oscillating circular cylinder in a uniform flow is measured by PIV to clarify the possible drag reduction on the circular cylinder and the physical mechanism of drag reduction at lower Reynolds number. The present results indicate that the width of the wake is reduced and the velocity fluctuations are suppressed in the wake of the circular cylinder, which result in the drag reduction rate of 30% at Reynolds number 2,000. It is found that the mechanism of the drag reduction is due to the periodic formation of small-scale vortices in the cylinder wake, which is caused by the complex interaction of the flow near the cylinder surface and the rotational oscillation of the circular cylinder near the unstable frequency of shear layer. The modification of the cylinder wake by the small-scale vortices is revealed in the cross-correlation contours between the velocity fluctuations, which support the drag reduction of the circular cylinder by rotational oscillation.

Acknowledgements

The authors would like to express gratitude to Prof. C. Arakawa of University of Tokyo, Dr. K. Srinivas of University of Sydney and Mr. Y. Tanahashi of Niigata University for their cooperation in this work.

References

Cheng, M., Chew, Y T. and Luo, S. C., Numerical Investigation of a Rotationally Oscillating Cylinder in Mean Flow, Journal of Fluids and Structures, 15 (2001), 981-1007.
Filler, J. R., Marston, P. L. and Mih, W. C., Response of the Shear Layers Separating from a Circular Cylinder to Small Amplitude Rotational Oscillations, Journal of Fluid Mechanics, 231 (1991), 481-499.
Fujisawa, N., Ikemoto, K. and Nagaya, K., Vortex Shedding Resonance from a Rotationally Oscillating Cylinder, Journal of Fluids and Structures, 12 (1998), 1041-1053.
Fujisawa, N. and Takeuchi, M., Flow Visualization and PIV Measurement of Flow Field around a Darrieus Rotor in Dynamic Stall, Journal of Visualization, 1 (1999), 379-386.
Fujisawa, N. and Takeda, G., Flow Control around a Circular Cylinder by Internal Acoustic Excitation, J. Fluids and Structures, 17 (2003), 903-913.
Griffin, O. M. and Hall, M. S., Review; Vortex Shedding Lock-in and Flow Control in Bluff Body Wakes, ASME Journal of Fluids Engineering, 113 (1991), 526-537.
He, J.-W., Glowinski, R., Metcalfe, R., Nordlander, A. and Periaux, J., Active Control and Drag Optimization for Flow past a Circular Cylinder, Journal of Computational Physics, 163 (2000), 83-117.
Hsiao, F. B. and Shyu, J. Y., Influence of Internal Acoustic Excitation upon Flow Passing a Circular Cylinder, Journal of Fluids and Structures, 5 (1991), 427-442.
Kim, K. C., Lee, M. B., Yoon, S. Y., Boo, J. S. and Chun, H. H., Phase Averaged Velocity Field in the Near Wake of a Square Cylinder Obtained by a PIV Method, Journal of Visualization, 5 (2002), 29-36.
Lu X. Y. and Sato, J., A Numerical Study of Flow past a Rotationally Oscillating Circular Cylinder, Journal of Fluids and Structures, 10 (1996), 829-849.
Okajima, A., Takata, H. and Asanuma, T., Viscous Flow around a Rotationally Oscillating Circular Cylinder, Report of Institute of Space and Aeronautical Science, University of Tokyo, 532 (1975).
Raffel, M., Willert, C. and Kompenhans, J., Particle Image Velocimetry, (1998), 105-146, Springer-Verlag, Berlin.
Shiels, D. and Leonard, A., Investigation of Drag Reduction on a Circular Cylinder in Rotary Oscillation, Journal of Fluid Mechanics, 431 (2001), 297-322.
Srinivas, K. and Fujisawa, N., Effect of Rotational Oscillation upon Fluid Forces about a Circular Cylinder, Journal of Wind Engineering and Industrial Aerodynamics, 91 (2003), 637-652.
Tokumaru, P. T. and Dimotakis, P. E., Rotary Oscillation Control of a Cylinder Wake, Journal of Fluid Mechanics, 224 (1991), 77-90.

Author profile

Nobuyuki Fujisawa: After graduating from Tohoku University (D.E. 1983), he joined Gunma University and worked as an associate professor since 1991. He has been a professor of Niigata University since 1997. He is interested in flow visualization, non-intrusive measurement and control of thermal and fluid flow phenomenon in engineering and science.

Masaru Ugata: He was educated at Niigata University (B.E. 2003). He is now working in Fujii corporation.

Tomokazu Suzuki: He was educated at Niigata University (B.E. 2000) and Graduate School of Niigata University (M.E. 2002). He is now working in Fuji Heavy Industries.